Functional Relationships of the Genetic Locus Encoding the Glycosyltransferase Enzymes Involved in Expression of the Lacto-N-neotetraose Terminal Lipopolysaccharide Structure in Neisseria Meningitidis

THE JOURNAL OF BIOLOGICAL CHEMISTRY
Vol. 271, No. 32, Issue of August 9, pp. 19166–19173, 1996

Printed in U.S.A.

Functional Relationships of the Genetic Locus Encoding the Glycosyltransferase Enzymes Involved in Expression of the Lacto-*N*-neotetraose Terminal Lipopolysaccharide Structure in *Neisseria meningitidis**

(Received for publication, April 4, 1996, and in revised form, May 21, 1996)

Warren Wakarchuk‡, Adèle Martin‡, Michael P. Jennings§¶, E. Richard Moxon§, and James C. Richards‡‖

From the ‡Institute for Biological Sciences, National Research Council of Canada, Ottawa, Ontario, K1A 0R6, Canada and the §Molecular Infectious Diseases Group and Department of Paediatrics, Institute for Molecular Medicine, John Radcliffe Hospital, Headington, Oxford, OX3 3DU, United Kingdom

The biosynthetic function of the *lgtABE* genetic locus of *Neisseria meningitidis* was determined by structural analysis of lipopolysaccharide (LPS) derived from mutant strains and enzymic assay for glycosyltransferase activity. LPS was obtained from mutants generated by insertion of antibiotic resistance cassets in each of the three genes *lgtA*, *lgtB*, *lgtE* of the *N. meningitidis* immunotype L3 strain ϕ3 MC58. LPS from the parent strain expresses the terminal lacto-*N*-neotetraose structure, Galβ1→4GlcNAcβ1→3Galβ1→4Glc. Mild hydrazine treatment of the LPS afforded *O*-deacylated samples that were analyzed directly by electrospray ionization mass spectrometry (ESI-MS) in the negative ion mode. In conjunction with results from sugar analysis, ESI-MS revealed successive loss of the sugars Gal, GlcNAc, and Gal in *lgt* B, *lgt* A, and *lgt* E LPS, respectively. The structure of a sample of *O*- and *N*-deacylated LPS derived by aqueous KOH treatment of *lgt* B LPS was determined in detail by two-dimensional homo- and heteronuclear NMR methods. Using a synthetic β-GlcNAc acceptor and a β-lactose acceptor, the glycosyltransferase activities encoded by the *lgtB* and *lgtA* genes were unambiguously established. These data provide the first definitive evidence that the three genes encode the respective glycosyltransferases required for biosynthesis of the terminal trisaccharide moiety of the lacto-*N*-neotetraose structure in *Neisseria* LPS. From ESI-MS data, it was also determined that the Gal-deficient LPS expressed by the *lgt* E mutant is identical to that of the major component expressed by immunotype L3 *galE*-deficient strains. The *galE* gene which encodes for UDP-glucose-4-epimerase plays an essential role in the incorporation of Gal into meningococcal LPS.

Diseases caused by *Neisseria meningitidis* remain a significant problem worldwide (1). Both capsule and lipopolysaccharide (LPS)[1] are recognized as major virulence determinants (2, 3) and, in the developed world, the group B capsular type is the leading cause of meningococcal meningitis (4). LPS comprises a heterogeneous mixture of molecules consisting of a variable core oligosaccharide (5–9) and a conserved lipid A component (10). On the basis of the structural diversity of the oligosaccharide epitopes and their reactivity with monoclonal antibodies, the meningococci have been classified into 12 immunotypes (11–13). Structural studies of core oligosaccharides and the use of monoclonal antibodies have led to the identification of both common and variable structural features which are responsible for immunotype specificity (13). In addition, terminal saccharide structures have been identified which are also found on the surface of human epithelial cells or in host secretions (14, 15). Included among these are Galα1→4Gal (immunotype L1), lacto-*N*-neotetraose (*e.g.* immunotypes L3 and L7), and lactose (*e.g.* immunotype L8) (16). Endogenous sialylation of the terminal galactosyl residue of the lacto-*N*-neotetraose epitope has also been demonstrated (9, 17). It is believed that the presence of these epitopes may facilitate the evasion of the host immune system (14). Phase variation in these terminal structures has been demonstrated (18), and recent virulence studies implicate differential expression of these terminal LPS epitopes in the pathogenesis of *N. meningitidis* (2, 19–21).

There has been increasing interest in the genetics of LPS expression in *Neisseria* (18, 22–25). Among the genes identified was meningococcal *galE* which encodes the UDP-glucose-4-epimerase essential for incorporation of galactose into LPS and an insertion mutant has been constructed in the *galE* gene which produces truncated LPS (22). The genetic locus responsible for expression of lacto-*N*-neotetraose, its terminally GalNAc-substituted analogue, and Galα1→4Gal in *Neisseria gonorrhoeae* LPS has been identified and characterized (25). In *N. meningitidis*, a gene locus named *lgtABE*, having homology to the gonococcal locus has been recently shown to be required for the biosynthesis of the terminal trisaccharide, Galβ1→4GlcNAcβ1→3Gal, of the lacto-*N*-neotetraose epitope

* This work was supported in part by the Programme Grants from the Medical Research Council UK, the Wellcome Trust, and Action Research. This is National Research Council of Canada Publication Number 39524. The costs of publication of this article were defrayed in part by the payment of page charges. This article must therefore be hereby marked "*advertisement*" in accordance with 18 U.S.C. Section 1734 solely to indicate this fact.

¶ Recipient of a Beit Memorial Research Fellowship. Present address: School of Biomolecular and Biomedical Science, Faculty of Science and Technology, Griffith University, Kessels Road, Nathan 4111, Queensland, Australia.

‖ To whom correspondence should be addressed: Institute for Biological Sciences, National Research Council Canada, 100 Sussex Dr., Ottawa, Ontario, K1A 0R6. Tel.: 613-990-0854; Fax: 613-941-1327; E-mail: RICHARDS@biologysx.lan.nrc.ca.

[1] The abbreviations used are: LPS, lipopolysaccharide; KDO, 3-deoxy-*D*-manno-octulosonic acid; PAGE, polyacrylamide gel electrophoresis; LPS-OH, *O*-deacylated LPS; GLC, gas-liquid chromatography; MS, mass spectrometry; ESI, electrospray ionization; NMR, nuclear magnetic resonance; COSY, correlated spectroscopy; NOE, nuclear Overhauser effect; NOESY, two-dimensional NOE spectroscopy; HMQC, heteronuclear multiple quantum coherence; PEA, phosphoethanolamine; FCHASE, 5-(fluorescein-carboxamido)-hexanoic acid succimidyl ester; CE, capillary electrophoresis; MES, 4-morpholineethanesulfonic acid.

and to provide the mechanism by which phase variable expression of the epitope is controlled (18). Mutants generated in each of three genes in the *lgtABE* locus were implicated by immunological and PAGE analysis of derived LPS to have a role in the synthesis of glycosyltransferase enzymes (18). In this study, the molecular structures for LPS produced by the three *lgt* mutant strains are determined providing, for the first time, definitive evidence that this genetic locus encodes the glycosyltransferases required for sequential addition of glycoses to the growing lacto-*N*-neotetraose end group. A relationship between the structures of the LPS elaborated by *lgt* E and *gal* E mutants is established. Moreover, the β-1,4-galactosyltransferase activity encoded by the *lgtB* gene and the β-1,3-*N*-acetylglucosaminyltransferase activity of the *lgtA* gene were unequivocally demonstrated by enzymic assay using synthetic acceptors.

EXPERIMENTAL PROCEDURES

Bacterial Strains—The following strains of *N. meningitidis* were used in this study: immunotype L7 strain M982B (NRCC no. 4725); *lgt* mutant strains ϕ3 *lgt* B, ϕ3 *lgt* A, and ϕ3 *lgt* E; and mutant strains MC58 *gal* E and H44/76 *gal* E. The insertional mutants containing a kanamycin-resistance (kan^r) cassette in each of the genes of the *lgtABE* locus were constructed from *N. meningitidis* immunotype L3 strain ϕ3 (MC58) as described previously (18). UDP galactose-deficient strains were constructed by insertion of kan^r cassette in the capsular polysaccharide biosynthetic locus copy of the *galE* gene of *N. meningitidis* MC58 and H44/76 (22).

Preparation of Lipopolysaccharide—N. meningitidis strains were resuscitated from microbeads on 5% sheep blood agar plates and incubated overnight at 37 °C, and the proceeds of six plates were suspended in 50 mL of Difco Bacto Todd Hewitt broth (Difco). For mutant strains, this culture was used to inoculate 2.5 liters of the same medium containing a final concentration of 50 μg/mL kanamycin (Sigma) and, following incubation at 37 °C for 6–8 h, was used to inoculate 60 liters of the above medium in a New Brunswick Scientific IF-75 fermenter. Fermenter growth was overnight (approximately 17 h) at 37 °C. The culture was killed by the addition of 1% (final concentration) phenol, chilled to 15 °C, and harvested by continuous centrifugation. Wet weight biomass yields were in the order of 3.5 g/liter. *N. meningitidis* strain M982B (immunotype L7) was grown under similar conditions as described previously (5). LPS was isolated by the hot phenol-water extraction procedure (26) and purified by repeated ultracentrifugation (105,000 × *g*, 4 °C, 2 × 5 h).

Deoxycholate-Polyacrylamide Gel Electrophoresis (PAGE)—Polyacrylamide gel electrophoresis was performed using the buffer system of Laemmli and Favre (27) as modified by Komuro and Galanos (28) with sodium deoxycholate as the detergent. Lipopolysaccharide bands were stained and visualized by silver staining as described by Tsai and Frasch (29).

Partial Acid Hydrolysis—LPS (25 mg) was hydrolyzed in 1% aqueous acetic acid (5 ml) for 2.5 h at 100 °C, the solution was then cooled (4 °C), and the precipitated lipid A was removed by low speed centrifugation. The supernatant solution was lyophilized, and the water-soluble component was fractionated on a Sephadex G-50 gel filtration column (2.0 × 90 cm, Pharmacia Biotech Inc.) by elution with pyridinium acetate (0.05 M, pH 4.5) to afford core oligosaccharide. The fractions were monitored for neutral glycoses (30) and KDO (31).

Preparation of O-Deacylated LPS—LPS was *O*-deacylated with anhydrous hydrazine under mild conditions as described previously (32). Briefly, a sample (14 mg) was treated with anhydrous hydrazine (1 mL) and stirred at 37 °C. After 1 h, the reaction mixture was cooled (0 °C) and hydrazine was destroyed by addition of cold acetone (5 ml). The precipitated product was washed with acetone (4 × 2 ml), acetone:water (4:1, 5 ml) and then lyophilized from water.

Preparation of O- and N-Deacylated LPS—Employing a modification of the method of Holst *et al.* (33), LPS (4 mg) was treated with hot alkali (4 M KOH, 18 h, 125 °C) to cleave ester- and amide-linked fatty acids. The reaction mixture was cooled to room temperature and neutralized (6 M HCl). Completely deacylated LPS was purified by gel filtration chromatography on a Sephadex G-10 column (1.6 × 90 cm, Pharmacia) eluted with pyridinium acetate (0.05 M, pH 4.5).

Analytical Methods—For analysis of constituent sugars, samples (0.5 mg each) of LPS or core oligosaccharide were hydrolyzed with 2 M trifluoroacetic acid for 1 h at 125 °C. The excess acid was removed by evaporation under a stream of nitrogen, and the glycoses were determined by gas-liquid chromatography-mass spectrometry (GLC-MS) of their derived alditol acetates as described previously (34). GLC-MS was performed with a Varian ion trap system fitted with a DB-17 fused silica capillary column (0.25 mm × 25 m, Quadrex Corp.) in the electron impact mode with a temperature program starting at 180 °C for 2 min followed by an increase of 5 °C/min to 300 °C.

Electrospray Ionization-Mass Spectrometry (ESI-MS)—Samples were analyzed in the negative or positive ion mode on a VG Quattro triple quadrupole mass spectrometer (Fisons Instruments) fitted with an electrospray ion source. Oligosaccharide samples were dissolved in water, this was diluted by 50% with acetonitrile:H_2O:MeOH:1% ammonia (4:4:1:1), and then the mixture was introduced by direct infusion at 4 μl/min with a Harvard syringe pump 22. The electrospray tip voltage was 3.5 kV, and the mass spectrometer was scanned from m/z 50–2500 with a scan time of 10 s. Data were collected in multichannel analysis mode, and data processing was handled by the VG data system (Masslynx). For MS-MS experiments, precursor ions were selected using the first quadrupole mass analyzer, and fragment ions, formed by collisional activation with argon in the rf-only quadrupole collision cell, were mass analyzed by scanning the third quadrupole. Collision energies were typically 60 eV.

Nuclear Magnetic Resonance (NMR) Spectroscopy—NMR spectra were obtained on a Bruker AMX 500 spectrometer using standard Bruker software. Measurements were made at 37 °C on solutions in 0.5 ml of D_2O subsequent to several lyophilizations with D_2O.

Proton NMR spectra were measured at 500 MHz using a spectral width of 6.0 KHz and a 90° pulse. Proton and ^{13}C chemical shifts were referenced to that of the methyl resonances of internal acetone (δ_H, 2.225 ppm; δ_C, 31.07 ppm). Two-dimensional homonuclear proton correlation experiments (COSY) (35) were measured over a spectral width of 2.3 or 1.3 KHz, using data sets ($t_1 \times t_2$) of 256 × 2048 or 512 × 2048 points; 32 or 64 scans were acquired, respectively. Spectra were processed in magnitude mode with symmetrization about the diagonal. Two-dimensional nuclear Overhauser effect experiments (NOESY) (36) were performed using a data set of 256 × 2048 points, a spectral width of 2.3 KHz, a 400 ms mixing time and 128 scans.

Heteronuclear two-dimensional ^1H-^{13}C chemical shifts correlations were measured in the ^1H-detected mode via multiple quantum coherence (HMQC) with proton decoupling in the ^{13}C domain (37), using data sets of 1024 × 256 points and spectral widths of 4.5 and 13.8 KHz for ^1H and ^{13}C domains, respectively; 128 scans were acquired for each t_1 value.

Phosphorous-31 spectra were measured at 202 MHz with a spectral width of 13 KHz and phosphoric acid (85%) was used as the external standard (δ_P, 0.0 ppm). ^1H-^{31}P correlations (HMQC) were made in the ^1H-detected mode by using a data matrix of 16 × 1024 points, sweep widths of 10 KHz for ^{31}P and 1.3 KHz for ^1H, and a mixing time of 60 ms.

Molecular Biology—Basic DNA manipulations were performed as described previously (38). A polymerase chain reaction was performed with *Pwo* polymerase as described by the manufacturer (Boehringer Mannheim). DNA sequencing was performed with an Applied Biosystems (ABI) model 370A automated DNA sequencer using the cycle sequencing kit from ABI. The expression vector used for the *lgtB* gene has been described previously (38).

Preparation of Fluorescein-labeled Aminophenylglycosides—p-Aminophenylglycoside (10 mg) (Sigma) was dissolved in 0.5 ml of 0.2 M triethylamine acetate buffer, pH 8.2. 5-(Fluorescein-carboxamido)-hexanoic acid succimidyl ester (10 mg, single iosmer) (FCHASE, Molecular Probes) was dissolved in 0.5 ml of methanol and added to the aminophenylglycoside solution. The mixture was stirred in the dark for 3 h at room temperature and then dried in a Savant Speedvac. The dry mixture was resuspended in 200 μl of 50% acetonitrile and spotted on a 1-mm thick 20 cm × 20-cm Silica 60 TLC plate (E. Merck). The TLC plate was developed with the following solvent system: ethyl acetate/methanol/water/acetic acid 7:2:1:0.1. After air drying in a fume hood, the bright yellow product was scraped off the plate and eluted with five 10-ml washes of distilled water. The water eluates were pooled, and the product was concentrated and desalted by binding to a Sep-Pak C_{18} reverse phase cartridge. After washing the cartridge with 20 ml of water, the product was eluted in 1–3 ml of 50% acetonitrile. The product was quantitated by spectrophotometry with $E^{494} = 68{,}000\ M^{-1}cm^{-1}$.

Capillary Electrophoresis—Capillary electrophoresis (CE) was performed with a Beckman P/ACE 5510 equipped with an Argon ion laser-induced fluorescence detector, λ = 488 nm. The capillary was a standard 75 μm × 50-cm bare silica, with the detector at 47 cm. The capillary was conditioned before each run by washing with 0.2 M NaOH

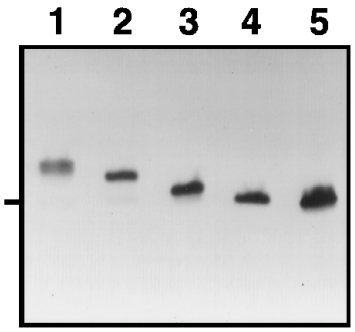

FIG. 1. **Silver-stained deoxycholate-PAGE of LPS (0.6 μg) from *N. meningitidis* M982B (immunotype L7) (*lane 1*) and MC58 (immunotype L3 strain ϕ3)-derived mutant strains, *lgt* B (*lane 2*), *lgt* A (*lane 3*), *lgt* E (*lane 4*), and *gal* E (*lane 5*).**

for 2 min, water for 2 min, then 20 mM sodium dodecyl sulfate/25 mM sodium tetraborate, pH 9.4, for 2 min. Samples were introduced by pressure injection for 2–5 s, and the separation was performed at 12 kV, 53 μA. Peak integration was performed with the Beckman System Gold (version 8) software.

Enzyme Assays—Cell extracts were prepared using an Avestin B3 Emulsiflex cell disrupter (Avestin Ottawa, Ontario). The clarified cell extracts were centrifuged at 100,000 × *g* for 1 h to pellet the cell membrane. Glycosyltransferase reactions were performed at 37 °C in 20-μl volumes and contained MES buffer 50 mM, pH 6.7, 10 mM $MnCl_2$, 5 mM dithiothreitol, 1.0 mM labeled acceptor, 1 mM UDP-Gal or 1 mM UDP-GlcNAc as donor, and various amounts of enzyme, either from crude bacterial extracts or extracts of recombinant *Escherichia coli* with the cloned *lgtB* gene. The reactions were terminated by the addition of an equal volume of 2% SDS and heated to 75 °C, for 3 min. These samples were then diluted appropriately in water prior to analysis by CE.

After the reaction the FCHASE-aminophenylglycosides were bound to a Sep-Pak C_{18} reverse phase cartridge, desalted by washing with water and then eluted in 50% acetonitrile. After drying under vacuum, the samples were dissolved in water, and glycosidase assays were performed as described by the enzyme manufacturer (Oxford Glycosystems). These samples were then diluted with water and again analyzed by CE.

RESULTS

Lacto-*N*-neotetraose-deficient mutant strains of *N. meningitidis* were constructed by insertion of kanamycin resistance cassettes into the *lgtABE* locus (mutants *lgt* A, *lgt* B, and *lgt* E) and the *galE* gene (mutant *gal* E) of the L3 immunotype strain (ϕ3) MC58 (18, 22). LPS was obtained from fermenter-grown cells by extraction with aqueous phenol (26) followed by ultracentrifugation of the dialyzed and concentrated aqueous phase. Meningococcal LPS, representative of the parent strain, has been reported (5) to be comprised of D-galactose (Gal), D-glucose (Glc), 2-amino-2-deoxy-*D*-glucose (GlcN), L-*glycero*-D-*manno*-heptose (Hep), and 3-deoxy-D-*manno*-octulosonic acid (KDO) in the molar ratio of 2:1:4:2:2. Compositional analysis of *lgt* B and *lgt* A LPS revealed the presence of these constituent sugars, but significantly less Gal was detected in both LPS samples as well as a diminished amount of GlcN in *lgt* A LPS. Quantitative analysis of the respective core oligosaccharides indicated the presence of equal molar amounts of Glc and Gal. Gal was not detected among the complete acid hydrolysis products of *lgt* E and *gal* E LPS indicating the absence of Gal in these LPS samples.

Deoxycholate-PAGE analysis of the LPS from the immunotype L3-derived mutants revealed single-band patterns that were faster migrating than meningococcal LPS containing the complete lacto-*N*-neotetraose epitope (Fig. 1). The observed electrophoretic mobilities of the bands correspond to low molecular weight LPS composed of a lipid A and a core oligosaccharide. LPS from *lgt* A, *lgt* B, and *lgt* E showed consecutively faster relative mobilities than that of immunotype L7 LPS

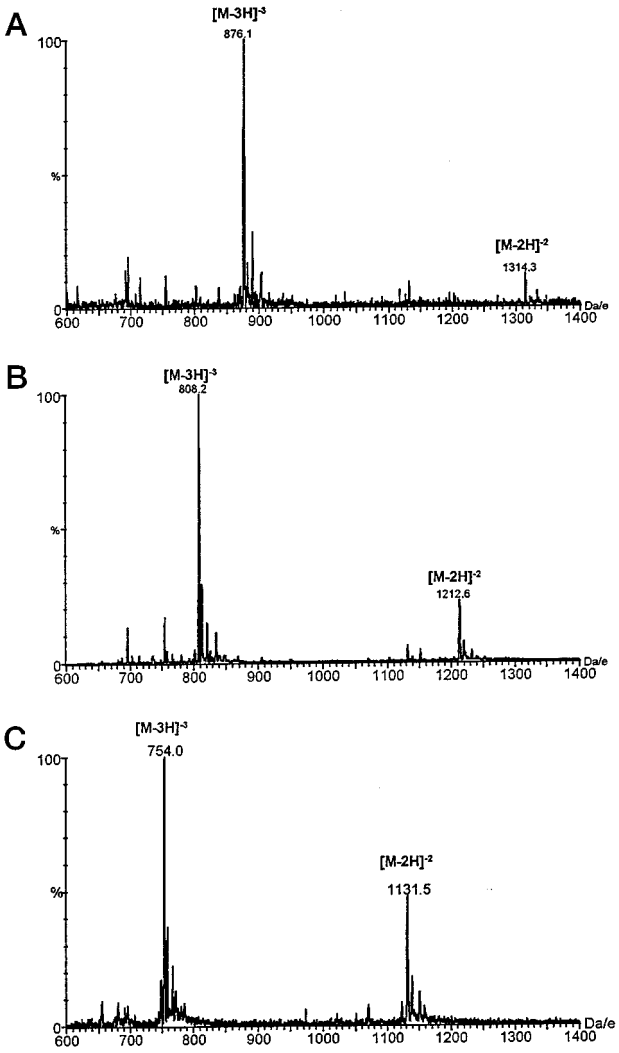

FIG. 2. **Negative ion ESI-MS of *O*-deacylated LPS from *N. meningitidis lgt* B (*A*), *lgt* A (*B*), and *lgt* E (*C*).** The calculated molecular masses and proposed structures are given in Table I. Low abundance peaks observed at $[M - 3H]^{3-} + 26$ and/or $[M - 3H]^{3-} + 13$ corresponding to M + *n* (39), where *n* = 1 or 2, may indicate adducts containing one or two potassium ions. Minor ions at $[M - 3H]^{3-} - 6$, observed particularly in spectrum C, represents $M - H_2O$ as previously observed for LPS-OH (39).

consistent with successive sugar deletions in the core oligosaccharide regions (Fig. 1). *gal* E LPS gave a more diffuse band that exhibited similar electrophoretic mobility to *lgt* E LPS. LPS from the *N. meningitidis* immunotype L7 strain M982B has been shown (9) to contain the immunotype L3 basal structure with complete expression of the lacto-*N*-neotetraose epitope.

Treatment of the LPS samples with anhydrous hydrazine under mild conditions afforded water-soluble *O*-deacylated samples that were suitable for mass spectral analysis by ESI. In the last few years, ESI-MS has proved to be a valuable tool for structural analysis and for probing structural heterogeneity of low molecular weight LPS (39–42). ESI-MS, recorded in the negative ion mode, for the *lgt* mutant *O*-deacylated LPS (LPS-OH) are shown in Fig. 2. For each sample, the mass spectrum is dominated by molecular peaks corresponding to doubly and triply deprotonated ions arising from a single molecular species and this is in agreement with the deoxycholate-PAGE results. For the *lgt* B LPS-OH sample (Fig. 2*A*), triply $[M - 3H]^{3-}$ and doubly $[M - 2H]^{2-}$ charged ions were observed at *m/z* 876.1 and *m/z* 1314.3, respectively. These data indicate that the

TABLE I
Negative ion ESI-MS data and proposed compositions for O-deacylated LPS of N. meningitidis MC58 lgt and gal E mutant strains

Mutant strain	Observed ion		Molecular mass		Proposed composition[b]
	$(M-3H)^{3-}$	$(M-2H)^{2-}$	Observed	Calculated[a]	
	m/z		*Da*		
lgt B	876.1	1314.3	2631.0	2631.4	$HexNAc_2{\cdot}Hex_2{\cdot}Hep_2{\cdot}PEA_1{\cdot}KDO_2{\cdot}$LipidA-OH
lgt A	808.2	1212.6	2427.4	2428.2	$HexNAc_1{\cdot}Hex_2{\cdot}Hep_2{\cdot}PEA_1{\cdot}KDO_2{\cdot}$LipidA-OH
lgt E	754.0	1131.5	2265.0	2266.1	$HexNAc_1{\cdot}Hex_1{\cdot}Hep_2{\cdot}PEA_1{\cdot}KDO_2{\cdot}$LipidA-OH
gal E	754.3	1132.0	2265.9	2266.1	$HexNAc_1{\cdot}Hex_1{\cdot}Hep_2{\cdot}PEA_1{\cdot}KDO_2{\cdot}$LipidA-OH

[a] Average mass units were used for calculation of molecular weight values based on proposed compositions as follows (39): HexNAc, 203.20; Hex, 162.14; Hep, 192.17; PEA, 123.05; KDO, 220.18; Lipid A-OH, 953.01.
[b] Sugar analysis indicates HexNAc corresponds to D-GlcNAc; Hex corresponds to one D-Glc and one D-Gal in *Igt* B and *Igt* A LPS, and to D-Glc only in *lgt* E and *gal* E LPS; and, Hep corresponds to L-glycero-D-manno heptose.

composition of the major *O*-deacylated LPS species (M_r 2631) contains one less hexose residue than that predicted for the complete lacto-*N*-neotetraose epitope of immunotype L7 LPS-OH (*i.e.* M_r 2793). The MS-MS spectrum of *lgt* B LPS-OH produced by low energy collisional activation of either the triply or doubly deprotonated ion afforded a major fragment ion at *m/z* 951 arising from cleavage of the KDO-β-glucosamine bond in which the ketosidic oxygen is retained by the *O*-deacylated lipid A forming a Y-type fragment ion (43) (data not shown). Cleavage of this linkage in LPS-OH to yield the *O*-deacylated lipid A singly charged ion appears to be the dominant fragmentation pathway in the negative ion mode (40, 42). The mass of this fragment is in accord with the proposed structure of *N. meningitidis* lipid A (10). The ESI-MS and MS-MS data are consistent with the *lgt* B LPS containing a truncated lacto-*N*-neotetraose chain (GlcN-Gal-Glc) attached to the basal inner core region of the molecule and this was confirmed by a detailed NMR analysis of the LPS backbone oligosaccharide (see below). ESI-MS analysis of *lgt* A and *lgt* E LPS-OH gave triply and doubly charged ions of lower mass (Fig. 2, *B* and *C*) corresponding to consecutive loss of hexosamine (GlcN) and a hexose (Gal) in the respective LPS samples. As expected (18, 22), the *gal* E LPS-OH sample gave an ESI-MS that was similar to that of *lgt E* (data not shown). In addition to this major LPS-OH species (M_r 2265.9), the ESI-MS of the *gal* E sample revealed a minor component (5–10% of the total) containing one extra hexose residue (M_r 2427.6) which was indicated to be Glc from sugar analysis. The ESI-MS data and the proposed compositions are summarized in Table I and the structural relationships are presented in Fig. 3.

Removal of ester and amido linked fatty acid groups of the *lgt* B LPS effected by treating it with strong alkali according to established procedures (33) afforded a backbone oligosaccharide sample. ESI-MS of the LPS backbone oligosaccharide sample, so obtained, in the negative ion mode revealed abundant triply $[M - 3H]^{3-}$ and doubly $[M - 2H]^{2-}$ charged ions at *m/z* 682.7 and 1024.5 corresponding to a decasaccharide trisphosphate ($Hex_2{\cdot}Hep_2{\cdot}HexN_4{\cdot}KDO_2{\cdot}(H_2PO_3)_3$) as the major molecular species (M_r 2051.2). Correspondingly, the sample gave ions at *m/z* 513.7, 684.7, and 1026.4 from $[M + 4H]^{4+}$, $[M + 3H]^{3+}$ and $[M + 2H]^{2+}$ multiply charged protonated ion species (M_r 2050.9) in the positive ion spectrum. MS-MS of the doubly deprotonated ion (*m/z* 1024.5) afforded a major fragment ion at *m/z* 499.1 from the glucosamine disaccharide bisphosphate derived from the lipid A portion of the molecule pointing to the presence of a single phosphate substituent in the core oligosaccharide region. A comparison of these results with the ESI-MS data obtained for *lgt* B LPS-OH (Table I) clearly indicates loss of ethanolamine from the PEA moiety, which is known to be substituted at O-3 of the penultimate heptose in immunotype L3 LPS (9). This most likely occurred under the alkaline KOH conditions used in the deacylation procedure. Elimination of ethanolamine accompanied by phosphate migration in *Haemophilus influenzae* LPS under these reaction conditions has been recently observed.[2]

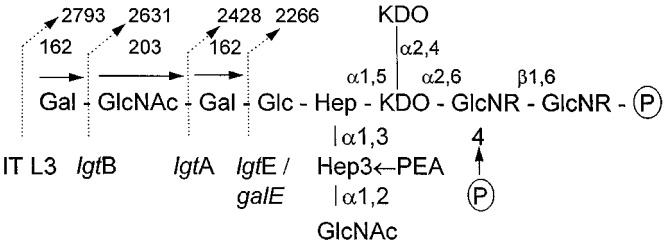

FIG. 3. **Structure of the lacto-*N*-neotetraose epitope in *N. meningitidis O*-deacylated LPS represented by immunotype L3 (*IT L3*) or L7 (9, 10).** See Fig. 6 for the position and configurations of the linkages of the lacto-*N*-neotetraose epitope. The positions at which this epitope is truncated in LPS of *lgt* B, *lgt* A, *lgt* E, and *gal* E mutants are indicated below the structure and the observed M_r are indicated above. Incremental mass values for consecutive sugar deletions is also indicated. The sequence of the sugar residues was confirmed for the fully deacylated *lgt* B LPS (present study).

The sequence of the glycose residues within the oligosaccharide component of the *lgt* B LPS was confirmed by NMR spectroscopy (45). This was achieved by measurement of nuclear Overhauser effects (NOEs) between protons on contiguous residues in the backbone oligosaccharide sample and required initial complete assignment of ring ^1H resonances.

As would be expected, the ^1H detected ^{13}C NMR spectrum of the backbone oligosaccharide derived from the *lgt* B LPS sample showed resonances in the low field region (90–105 ppm), corresponding to the anomeric carbons from eight aldose residues. In addition, diagnostic signals from the methylene carbons of two KDO residues were observed at 35.1 and 35.7 ppm. The ^1H NMR spectrum showed characteristic resonances (34, 46) in the high field region from the H-3 methylene protons from the two α-linked-KDO residues at 1.84 ppm (*t*, 1H, H-3ax), 2.00 ppm (*t*, 1H, H-3′ax) and 2.15 ppm (m, 2H, H-3eq/H-3′eq). The low field region of the ^1H spectrum (5.8–4.4 ppm) was complex indicating the sample to be a mixture of two related decasaccharides. The anomeric region of the two-dimensional ^1H-^{13}C correlation map was especially revealing since a doubling of anomeric ^1H signals from several residues in the inner core oligosaccharide region was readily discernable (Fig. 4). An approximate 60/40 ratio of two decasaccharides is indicated from estimation of the area of related anomeric ^1H signals, *e.g.* α-GlcN anomeric protons at 5.42/5.40 ppm. The proton resonances were assigned by two-dimensional homonuclear correlation (COSY) (45) and the component monosaccharide units were identified from the ^1H chemical shift (9, 47) and coupling constant values (48). The chemical shift data (Table II) is consistent with each D-sugar residue being present in the pyr-

[2] H. Masoud, E. R. Moxon, A. Martin, and J. C. Richards, unpublished results.

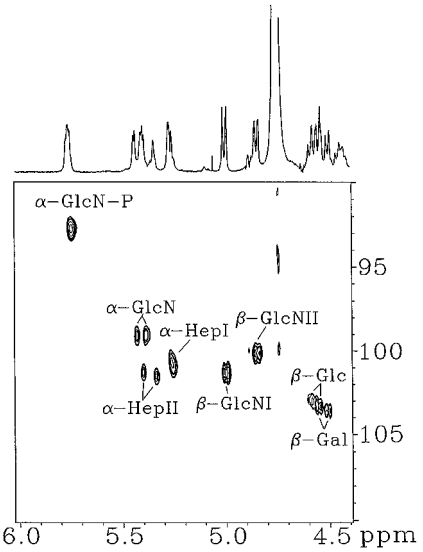

FIG. 4. **Heteronuclear two-dimensional ^{1}H-^{13}C chemical shift correlation map of the anomeric region of the *lgt* B deacylated LPS oligosaccharide sample.** Assignments of the glycose residues are indicated.

anosyl ring form. Further evidence for this was obtained from intraresidue NOE data (Table III) which also served to confirm the anomeric configurations of the linkages.

Proton spin-systems corresponding to the monomeric components from an α-glucosamine (α-GlcN), two heptoses (α-HepI, α-HepII), a β-glucose (β-Glc), and a β-galactose (β-Gal) in each of the two decasaccharides were identified (Table II). In addition to the two KDO residues, unique single spin-systems were identified for the two glucosamine residues in the deacylated lipid A region (α-GlcN-P, β-GlcNII) and for the terminal β-linked glucosamine (β-GlcNI). Correlation of the H-2 resonances with the directly attached ^{13}C resonances (HMQC experiment), which occurred in the ^{13}C-chemical shift region (50−60 ppm) diagnostic of amino substituted carbons, confirmed the identity of the GlcN residues.

A comparison of the ^{1}H NMR data for the residues listed in Table II revealed significant differences in chemical shifts and coupling patterns for the ^{1}H resonances associated with the residues assigned to α-HepII. This was readily apparent from the downfield shifted values for α-HepII H-3 (4.41 ppm, $^{3}J_{H,p} \sim$ 10 Hz) and α-HepII* H-4 (4.45 ppm, $^{3}J_{H,p} \sim$ 10 Hz), and is attributed to phosphate substitution at different sites in the two oligosaccharides. In the ^{31}P NMR spectrum, three signals were observed at 1.37, 0.55 and −1.84 ppm, of which the latter two showed strong correlations in the ^{1}H-^{31}P correlation experiment to H-4 of β-GlcNII and H-1 of α-GlcN-P, respectively, confirming the presence of monophosphate groups at the corresponding positions in the GlcNβ1→6GlcN moiety. As expected for the deacylated oligosaccharide derived from the parent strain LPS (9), a strong correlation was observed between α-HepII H-3 (4.41 ppm) and one of the ^{31}P resonances (0.55 ppm) in the ^{1}H-^{31}P correlation map indicating substitution by phosphate of the C-3 position. In the related oligosaccharide, the phosphate substituent is located at the C-4 position of the heptose as indicated by the occurrence of a strong correlation between α-HepII* H-4 (4.45 ppm) and the ^{31}P signal at 1.37 ppm.

The two decasaccharides were shown to have identical sugar residue sequences from transglycosidic NOE measurements. NOE connectivities were observed between anomeric and aglyconic protons on contiguous residues (Table III). Thus, the occurrence of NOEs between the proton pairs β-GlcNI H-1/β-Gal H-3, β-Gal H-1/β-Glc H-4, β-Glc H-1/α-HepI H-4, and α-HepI/KDOI H-5 established the partial sequence of the main chain: GlcNIβ1→3Galβ1→4Glcβ1→4HepIα1→5KDOI.

In *N. meningitidis* LPS (5), HepI forms a branch point to which the disaccharide GlcNα1 → 2HepII is attached. This was confirmed for *lgt* B LPS from the observed NOEs between α-GlcN H-1/α-HepII H-2 and α-HepII H-1/α-HepI H-3 protons. KDO in the main chain (KDOI) is known (49, 50) to be substituted at O-4 by a second unit (KDOII) and to link the core oligosaccharide to the putative *O*-deacylated lipid A. The ^{1}H NMR and ESI-MS data is in accord with this inference and, as expected, a transglycosidic NOE is observed between H-1of β-GlcNII and the H-6/H-6′ proton pair of α-GlcN-P in the deacylated lipid A region. The structures of the two decasaccharides are depicted in Table II.

Glycosyltransferase activity of the *lgtB* gene was established using a fluorescence-labeled synthetic acceptor in a capillary electrophoresis-based assay. Cell extracts of MC58 (L3 immunotype strain φ3) and the *lgt* B mutant were used in glycosyltransferase assays with FCHASE-aminophenyl-β-GlcNAc as an acceptor molecule. Capillary electrophoresis analysis of the reaction mixture from MC58 is shown in Fig. 5. Three major peaks were observed in the reaction mixture from MC58. The fastest migrating peak (*peak 1*) was identified as FCHASE-aminophenyl-β-LacNAc as its migration time (12.9 min.) is identical to authentic FCHASE-β-LacNAc (data not shown). In addition, this peak is sensitive to β-galactosidase as shown in Fig. 5*B*. The second peak having a migration time of 13.1 min corresponded to FCHASE-aminophenyl-β-GlcNAc. The third peak at 14.6 min results from the action of an endogenous hexosaminidase activity present in the extracts. The appearance of *peak 2* was dependent on the addition of UDP-Gal and $MnCl_2$ to the reaction mixture and the presence of β-linked GlcNAc as an acceptor. This same enzyme activity could be expressed in *E. coli* carrying the *lgt* B gene in an expression vector (data not shown). The cell extracts of the *lgt* B mutant strain failed to catalyze addition of β-Gal to the GlcNAc acceptor (data not shown).

A similar analysis was performed for the function of the *lgtA* gene. Cell extracts of MC58 had β-*N*-acetylglucosaminyltransferase activity when FCHASE-aminophenyl-β-lactose was used as an acceptor and UDP-GlcNAc was used as a donor. The product peak from this reaction was also shown to be sensitive to β-*N*-acetylhexosamidase (data not shown). Cell extracts of the *lgt* A mutant were unable to transfer β-GlcNAc to the lactose acceptor.

DISCUSSION

The *lgtABE* genetic locus is required for the biosynthesis of the lacto-*N*-neotetraose terminal LPS structure in *N. meningitidis* (18). Insertion mutants have been constructed in each of the three genes in the *lgtABE* locus of the immunotype L3 strain (φ3) of MC58. In previous work, immunological and PAGE analysis of LPS from mutants *lgt* B, *lgt* A, and *lgt* E suggested structural alterations in lacto-*N*-neotetraose epitope, but the determination of the chemical structures of the LPS core oligosaccharide regions had not been reported. To unequivocally assign functions to *lgtABE* locus, determination of the detailed structure of the LPS core oligosaccharide regions was necessary. In this study, the complete molecular structure of deacylated *lgt* B LPS was determined by electrospray mass spectrometry and detailed NMR analytical methods. A structural model from this LPS is shown in Fig. 6.

The structure of the *N. meningitidis* immunotype L3 LPS has been determined in detail (9). In complete expression of the L3 immunotype, the terminal β-galactose of the lacto-*N*-neotetraose epitope is capped by α-2,3-linked sialic acid residues.

TABLE II

Proton chemical shifts and coupling constants for the deacylated backbone oligosaccharides derived from N. meningitidis lgt B LPS

Observed first-order chemical shifts and ring proton coupling constants (±0.5 Hz) measured at 37 °C in D_2O.

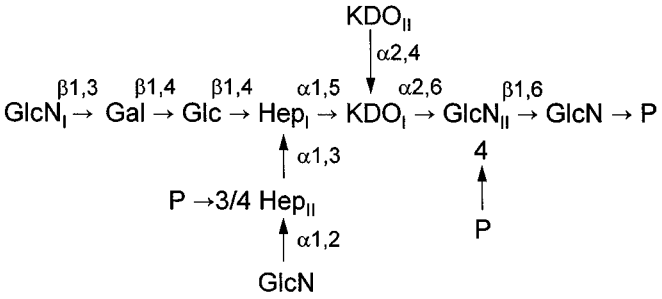

Proton resonance	Core oligosaccharide residue assignments[a]								Deacylated lipid A residue assignments	
	β-GlcNI	β-Gal	β-Glc	α-HepI	α-HepII	α-GlcN	KDOI	KDOII	β-GlcNII	α-GlcN-P
H-1	5.00	4.54 4.50	4.58 4.59	5.29 5.28	5.41 5.32	5.42 5.40			4.84	5.75
($J_{1,2}$)	(8.1)	(8.9)	(8.9) (8.9)	(<3) (<3)	(<3) (<3)	(3.8) (3.8)			(8.2)	(—)[b]
H-2	3.12	3.71 3.72	3.48 4.43	4.12 4.15	4.53 4.38	3.38 3.38			3.16	3.48
($J_{2,3}$)	(9.9)	(10.0)	(9.3) (9.5)	(—) (—)	(~3) (~3)	(9.6) (9.6)			(9.6)	(10.0)
H-3	3.70	3.90	~3.64 3.69	4.09 4.11	4.41 4.25	3.92 3.99	2.00/2.15[c]	1.84/2.15[c]	3.91	3.92
($J_{3,4}$)	(10.5)	(3.4)	(—) (9.8)	(—) (—)	(10.5,10.0[d])(10.1)	(9.9)(10.0)	—	(—)	(10.2)	(10.1)
H-4	3.50	4.19	~3.64 3.59	4.29 4.25	4.08 4.45	3.59 3.52	4.22	—	3.95	3.62
($J_{4,5}$)	(—)	(~1)	(—) (—)	(—) (—)	(9.0) (9.8, 10.0[d])	(~10) (10.0)	(—)		(—)	(9.9)
H-5	3.51	3.71	3.53 3.60	4.18 4.28	3.81 3.82	3.89 3.90	4.28	—	3.63	4.15
H-6	—[e]	~3.80[f]		4.08 4.10	——	——	—	—	4.12	3.81/4.29[f]
H-7				——	——		3.85	—		
H-8							—	—		

[a] Data recorded on the *left* are for the decasaccharide corresponding to the LPS backbone oligosaccharide (9). Data on the *right* are for proton resonances shifted (≥0.01 ppm) in the decasaccharide which carries a phosphate substitute at the O-4 position in α-HepII.

[b] (—), coupling constant value not determined.

[c] H-3 (ax) and H-3 (eq) value, respectively.

[d] Value for $^3J_{H,P}$.

[e] —, chemical shift unresolved.

[f] H-6 and H-6′ value.

TABLE III

Proton NOE data for the deacylated backbone oligosaccharides derived from N. meningitidis lgt B LPS

Measured from NOESY experiment. Residues indicated by an asterisk are from the decasaccharide which carries a phosphate substitute at the O-4 position in α-HepII.

Anomeric proton	Observed proton		Partial sequence
	Intraresidue NOE	Transglycosidic NOE	
ppm		*ppm*	
5.00 (β-GlcNI)	3.70 (H-3), 3.51 (H-5)	3.90 (H-3 of β-Gal)	GlcNIβ1→3Gal
4.54 (β-Gal)	3.90 (H-3), 3.71 (H-5)	3.64 (H-4 of β-Glc)	Galβ1→4Glc
4.50 (β-Gal*)	3.90 (H-3), 3.71 (H-5)	3.59 (H-4 of β-Glc*)	
4.58 (β-Glc)	3.64 (H-3), 3.53 (H-5)	4.29, 4.08 (H-4, H-6 of α-HepI)	Glcβ1→4HepI
4.59 (β-Glc*)	3.69 (H-3), 3.60 (H-5)	4.25, 4.10 (H-4, H-6 of α-HepI*)	
5.29 (α-HepI)	4.12 (H-2)	4.27 (H-5 of α-KDOI)	HepIα1→5KDOI
5.28 (α-HepI*)	4.15 (H-2)	4.28 (H-5 of α-KDOI*)	
5.42 (α-GlcN)	3.38 (H-2)	4.53 (H-2 of α-HepII)	GlcNα1→2HepII
5.40 (α-GlcN*)	3.38 (H-2)	4.38 (H-2 of α-HepII*)	
5.41 (α-HepII)	4.53 (H-2)	4.09, 4.12 (H-3, H-2 of α-HepI)	HepIIα1→3HepI
5.32 (α-HepII*)	4.38 (H-2)	4.11, 4.15 (H-3, H-2 of α-HepI*)	
4.84 (β-GlcNII)	3.91 (H-3), 3.63 (H-5)	4.29, 3.81 (H-6′, H-6 of α-GlcN-P)	GlcNIIβ1→6GlcN-P
5.75 (α-GlcN-P)	3.48 (H-2)		

LPS of other *N. meningitidis* immunotypes, notably L7, also express the lacto-*N*-neotetraose epitope, but not the sialylated variant. LPS from *lgt B* only differs from that of the L7 immunotype in that it lacks the terminal β-galactose residue of the lacto-*N*-neotetraose epitope (9) and this is consistent with the observed inability of this mutant strain to bind the type-specific L3 monoclonal antibody Mn4A8-B2 (18). A comparison of *O*-deacylated LPS derived from *lgt* B with those from *lgt* A and *lgt* E by ESI-MS revealed further sugar truncations in the lacto-*N*-neotetraose epitope arising from respective loss of β-GlcNAc and β-GlcNAc-β-Gal residues. It was further established that the *lgt* E LPS is identical to the major LPS component expressed by the *gal* E mutant, a galactose deficient LPS resulting from inactivation of UDP-Glc-4-epimerase which is required for synthesis of UDP-Gal (22).

The structural data for the mutant LPS clearly indicate that the *lgtABE* locus encodes the glycosyltransferases for the biosynthesis of lacto-*N*-neotetraose terminal epitope. A mutation in the *lgtE* gene affords the truncated LPS containing a 1,4-linked β-Glc terminal group attached to α-HepI. The *lgt* A mutant which contains a functional *lgtE* gene is capable of adding β-Gal in a 1,4-linkage to this β-Glc to form the terminal lactose structure. Thus, the *lgtE* gene encodes for a β-galactosyltransferase. It is worthy to note that the structure of the *lgt*

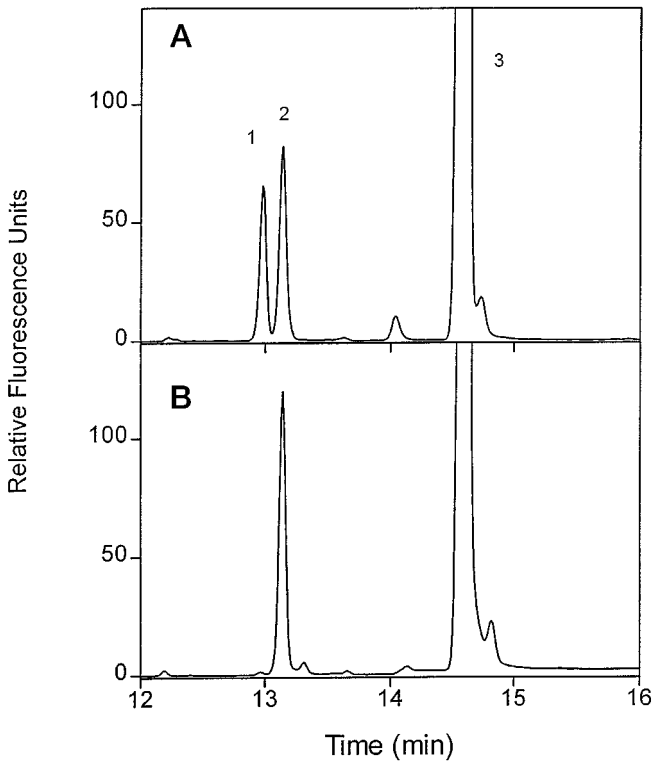

FIG. 5. **Capillary electrophoresis analysis of the reaction mixture from *N. meningitidis* MC58 (immunotype L3 strain ϕ3) after 3 h incubation with FCHASE-aminophenyl-β-GlcNAc (*A*) and following subsequent treatment of the reaction mixture with β-galactosidase (*B*).** *Peak 1*, FCHASE-aminophenyl-β-LacNAc; *peak 2*, FCHASE-aminophenyl-β-GlcNAc; *peak 3*, FCHASE-aminophenol.

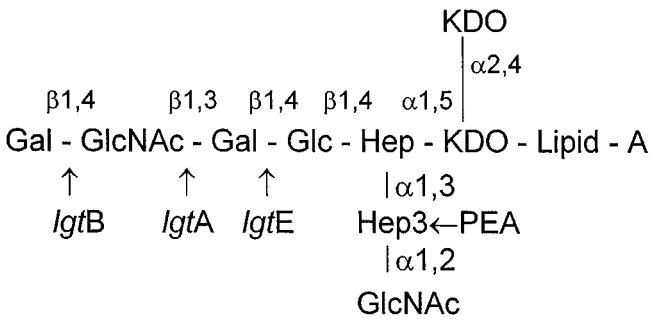

FIG. 6. **Structure of the LPS core oligosaccharide regions of meningococcal immunotype L3 and of derived *lgt* B, *lgt* A, and *lgt* E mutants.** The glycosyltransferase functions encoded by the genes in the *lgtABE* locus are indicated by the *arrows*.

A mutant LPS is identical to that elaborated by immunotype L8 (5). Correspondingly, the *lgt* B mutant containing a functional *lgtA* gene is capable of adding β-GlcNAc in a 1,3-linkage to the terminal β-Gal of the lactose epitope. It follows that the *lgtA* gene encodes the specific β-*N*-acetylglucosamine transferase for synthesis of the GlcNAcβ1→3Gal terminal unit. Finally, the parent immunotype L3 strain (MC58), which contains a functional *lgtB* gene, is capable of elaborating the complete lacto-*N*-neotetraose unit which indicates that this gene encodes the β-galactosyltransferase for catalyzing addition of the 1,4-linked β-Gal to the terminal β-GlcN. The function of this gene was firmly established by demonstrating β-galactosyltransferase enzyme activity with a synthetic β-GlcNAc acceptor. Correspondingly, the β-*N*-acetylglucosaminyltransferase activity encoded by *lgtA* was confirmed with a synthetic β-lactose acceptor, whereas experiments to assay transferase activity of the *lgtE* gene using a synthetic β-Glc acceptor were unsuccessful. It is likely that the latter enzyme has a more stringent acceptor specificity and requires β-Glc linked to heptose, precluding recognition of our synthetic acceptor.

Identification and characterization of the *lgt* genetic locus was first reported (25) in *N. gonorrhoea* and it was postulated that the genes within the locus encoded for glycosyltransferases involved in the biosynthesis of lacto-*N*-neotetraose and its GalNAc containing analogue in gonococcal LPS. In meningococci, the *lgtABE* locus contains three genes which are homologous to the gonococcal *lgtA*, *lgtB*, and *lgtE* genes (18). The role of these genes in meningococcal LPS phase variation has been demonstrated (18) and it was recently shown (51) that LPS phase variation in *N. gonorrhoea* occurs by a similar genetic mechanism. The evidence presented in the present study unequivocally demonstrates the glycosyltransferase functions of this *Neisserial* gene locus. The site where the specific transferases function in the biosynthesis of the lacto-*N*-neotetraose epitope is shown in Fig. 6.

Recently Lee *et al.* (52) reported that a meningococcal *gal* E mutant (strain NMB-SS3) expresses glycosyltransferase activity capable of adding one or two additional glucose residues to the immunotype L2 inner core LPS structure, and it was suggested that this provided an alternative biosynthetic pathway to the normal wild-type lacto-*N*-neotetraose structure. The structure of the LPS of immunotype L2 is similar to that of immunotype L3 in that it contains the lacto-*N*-neotetraose oligosaccharide epitope and the sialylated analogue, but differs in the inner core region where it contains an additional α-Glc moiety that is 1,3-linked to HepII (8). In the present study, the *gal* E mutant of immunotype L3 (strains MC58 and H44/76) produced, in addition to the expected LPS, ($GlcNAc_1{\cdot}Glc_1{\cdot}Hep_2{\cdot}PEA_1{\cdot}KDO_2{\cdot}$LipidA), a minor amount of a second LPS species containing one additional glucose (<10% by ESI-MS).[3] The extra glucose containing species, $GlcNAc_1{\cdot}Glc_2{\cdot}Hep_2{\cdot}PEA_1{\cdot}KDO_2{\cdot}$LipidA, was not detectable by ESI-MS in the LPS-OH sample obtained from the *lgt* E mutant, a strain known to contain a mutation in a single gene (22); only the $GlcNAc_1{\cdot}Glc_1{\cdot}Hep_2{\cdot}PEA_1{\cdot}KDO_2{\cdot}$LipidA-OH species was observed (Figs. 2*C* and 3). These data are consistent with either the galactosyltransferase encoded by the *lgtE* gene possessing the capability to mediate the addition of β-Glc to the Glcβ1→4HepI acceptor at low levels, or the presence of a meningococcal glycosyltransferase which manifests itself when there is a build up of this acceptor.

Mutational analysis of genes involved in LPS biosynthesis has involved examination of changes in the LPS reactivity with monoclonal antibodies, their migration patterns on PAGE and, in some cases, measurement of radioactive sugar incorporation into endogenous LPS glycosyltransferase acceptors (22, 25, 44). Very little data exist on the measurement of glycosyltransferase activity involved in LPS biosynthesis. Our enzymatic assay of β-1,4-galactosyltransferase activity with the parent MC58 ϕ3, the *lgt* B mutant, and the recombinant *E. coli* expressing *lgtB* unequivocally demonstrates this gene encodes a β-1,4-galactosyltransferase which requires a β-linked GlcNAc as an acceptor. To the best of our knowledge, this represents the first correlation of a proposed bacterial glycosyltransferase

[3] ESI-MS and sugar analysis of LPS-OH from a meningococcal *gal* E mutant derived from immunotype L2 ($35E_3$, constructed by insertion of kan^r cassette into the *galE* gene of strain 35E (22), gave the expected species, $GlcNAc_1{\cdot}Glc_2{\cdot}Hep_2{\cdot}PEA_1{\cdot}KDO_2{\cdot}$LipidA-OH ($M_r$ 2427.6) as the major component, together with a small amount (~10%) of the species containing one additional glucose (M_r 2589.9). At variance with results reported for strain NMB-SS3 (52), LPS-OH species containing further additions of glucose residues were not detectable (A. Martin, D. Krajcarski, and J. C. Richards, unpublished results).

gene with that enzymatic activity using a synthetic glycosyltransferase acceptor. We are now in the process of characterizing this enzyme.

Acknowledgments—We thank D. W. Griffith for large-scale production of cells, N. Eichler for isolation of LPS, F. Cooper for GLC-MS analyses, D. Krajcarski for ESI-MS, and A. Cunningham for CE analyses. We also thank Dr. H.J. Jennings for providing us with an authentic sample of *N. meningitidis* immunotype L7, and Dr. H. Masoud for helpful discussions.

REFERENCES

1. Peltola, H. (1983) *Rev. Infect. Dis.* **5**, 71–91
2. Jones, D. M., Borrow, R., Fox, A. J., Gray, S. & Cartwright, K. A. (1992) *Microb. Pathog.* **13**, 219–224
3. Griffiss, J. M., Schneider, H., Mandrell, R. E., Yamasaki, R., Jarvis, G. A., Kim, J. J., Gibson, B. W., Hamadeh, R. & Apicella, M. A. (1988) *Rev. Infect. Dis.* **10**, 287–295
4. Peltola, H., Mäkelä, P. H. & Käyhty, H. (1977) *N. Engl. J. Med.* **297**, 686–691
5. Jennings, H. J., Johnson, K. G. & Kenne, L. (1983) *Carbohydr. Res.* **121**, 233–241
6. Di Fabio, J. L., Michon, F., Brisson, J.-R. & Jennings, H. J. (1990) *Can. J. Chem.* **68**, 1029–1034
7. Michon, F., Beurret, M., Gamian, A., Brisson, J.-R. & Jennings, H. J. (1990) *J. Biol. Chem.* **265**, 7243–7247
8. Gamian, A., Beurret, M., Michon, F., Brisson, J.-R. & Jennings, H. J. (1992) *J. Biol. Chem.* **267**, 922–925
9. Pavliak, V., Brisson, J.-R., Michon, F., Uhrin, D. & Jennings, H. J. (1993) *J. Biol. Chem.* **268**, 14146–14152
10. Kulshin, V. A., Zähringer, U., Lindner, B., Jäger, K., Dmitriev, B. A. & Rietschel, E. T. (1991) *Eur. J. Biochem.* **198**, 697–704
11. Zollinger, W. D. & Mandrell, R. E. (1977) *Infect. Immun.* **18**, 424
12. Zollinger, W. D. & Mandrell, R. E. (1980) *Infect. Immun.* **28**, 451–458
13. Verheul, A. F. M., Snippe, H. & Poolman, J. T. (1993) *Microbiol. Rev.* **57**, 34–49
14. Mandrell, R. E., Griffiss, J. M. & Macher, B. A. (1988) *J. Exp. Med.* **168**, 107–126
15. Virji, M., Weiser, J. N., Lindberg, A. A. & Moxon, E. R. (1990) *Microb. Pathog.* **9**, 441–450
16. Scholten, R. J. P. M., Kuipers, B., Valkenberg, H. A., Dankert, J., Zollinger, W. D. & Poolman, J. T. (1994) *J. Med. Microbiol.* **41**, 236–243
17. Tsai, C.-M. & Civin, C. I. (1991) *Infect. Immun.* **59**, 3604–3609
18. Jennings, M. P., Hood, D. W., Peak, I. R. A., Virji, M. & Moxon, E. R. (1995) *Mol. Microbiol.* **18**, 729–740
19. Weiner, S. J., Kollman, P. A., Case, D. A., Singh, U. C., Ghio, C., Alagona, G., Profeta, S., Jr. & Weiner, P. (1984) *J. Am. Chem. Soc.* **106**, 765–784
20. Moran, A. P. (1995) *J. Toxicol.* **14**, 47–83
21. Virji, M., Makepeace, K., Peak, I., Ferguson, D. J. P., Jennings, M. P. & Moxon, R. E. (1995) *Mol. Microbiol.* **18**, 741–755
22. Jennings, M. P., van der Ley, P., Wilks, K. E., Maskell, D. J., Poolman, J. T. & Moxon, R. E. (1993) *Mol. Microbiol.* **10**, 361–369
23. Robertson, B. D., Frosch, M. & van Putten, J. P. M. (1993) *Mol. Microbiol.* **8**, 891
24. Zhou, D., Stephens, D. S., Gibson, B. W., Engstrom, J. J., McAllister, C. F., Lee, F. K. & Apicella, M. A. (1994) *J. Biol. Chem.* **269**, 11162–11169
25. Gotschlich, E. (1994) *J. Exp. Med.* **180**, 2181–2190
26. Westphal, O. & Jann, K. (1965) *Methods Carbohydr. Chem.* **5**, 83–91
27. Laemmli, U. K. & Favre, M. (1973) *J. Mol. Biol.* **80**, 575–599
28. Komuro, T. & Galanos, C. (1988) *J. Chromatogr.* **450**, 381–387
29. Tsai, C.-M. & Frasch, C. E. (1982) *Anal. Biochem.* **119**, 115–119
30. Dubois, M., Gilles, K. A., Hamilton, J. K., Rebers, P. A. & Smith, F. (1956) *Anal. Chem.* **28**, 350–356
31. Aminoff, D. (1965) *Biochem. J.* **81**, 384–392
32. Holst, O., Brade, L., Kosma, P. & Brade, H. (1991) *J. Bacteriol.* **173**, 1862–1866
33. Holst, O., Broer, W., Thomas-Oates, J. E., Mamat, U. & Brade, H. (1993) *Eur. J. Biochem.* **214**, 703–710
34. York, W. S., Darvill, A. G., McNeil, M. & Albersheim, P. (1985) *Carbohydr. Res.* **138**, 109–126
35. Bax, A., Freeman, R. & Morris, G. (1981) *J. Magn. Reson.* **42**, 164–168
36. Kumar, A., Ernst, R. R. & Wüthrich, K. (1980) *Biochem. Biophys. Res. Commun.* **95**, 1–6
37. Bax, A. (1983) *J. Magn. Reson.* **52**, 330–334
38. Wakarchuk, W. W., Campbell, R. L., Sung, W. L., Davoodi, J. & Yaguchi, M. (1994) *Protein Sci.* **3**, 467–475
39. Gibson, B. W., Melaugh, W., Phillips, N. J., Apicella, M. A., Campagnari, A. A. & Griffiss, J. M. (1993) *J. Bacteriol.* **175**, 2702–2712
40. Auriola, S., Thibault, P., Sadovskaya, I., Altman, E., Masoud, H. & Richards, J. C. (1996) in *Biochemical and Biotechnological Applications of Electrospray Ionization Mass Spectrometry* (Snyder, P. A. ed) pp. 149–165, American Chemical Society, Washington, D. C.
41. Gibson, B. W., Phillips, N. J., Melaugh, W. & Engstrom, J. J. (1996) in *Biochemical and Biotechnological Applications of Electrospray Ionization Mass Spectrometry* (Snyder, A. P. ed) pp. 166–184, American Chemical Society, Washington, D. C.
42. Kelly, J., Masoud, H., Perry, M. B., Richards, J. C. & Thibault, P. (1996) *Anal. Biochem.* **233**, 15–30
43. Domon, B. & Costello, C. E. (1988) *Glycoconj. J.* **5**, 397–409
44. Schnaitman, C. A. & Klena, J. D. (1992) *Microbiol. Rev.* **57**, 655–682
45. Masoud, H., Altman, E., Richards, J. C. & Lam, J. S. (1994) *Biochem.* **33**, 10568–10578
46. Carlson, R. W., Hollingsworth, R. L. & Dazzo, F. B. (1988) *Carbohydr. Res.* **176**, 127–135
47. Bock, K. & Thogersen, H. (1982) *Annu. Rep. NMR Spec.* **13**, 1–57
48. Altona, C. & Haasnoot, C. A. G. (1980) *Organ. Magn. Reson.* **13**, 417–429
49. Raetz, C. R. H. (1990) *Annu. Rev. Biochem.* **59**, 129–170
50. Holst, O. & Brade, H. (1992) in *Bacterial Endotoxic Lipopolysaccharides* (Morrison, D. C. ed) pp. 135–170
51. Yang, Q. L. & Gotschlich, E. C. (1996) *J. Exp. Med.* **183**, 323–327
52. Lee, F. K. N., Stephens, D. S., Gibson, B. W., Engstrom, J. J., Zhou, D. & Apicella, M. A. (1995) *Infect. Immun.* **63**, 2508–2515